

# Flexural vibrations of a monopolar domain wall in yttrium iron garnet

L. M. Dedukh, V. I. Nikitenko, and V. T. Synogach

*Institute of Solid State Physics, USSR Academy of Sciences*

(Submitted 3 March 1988)

Zh. Eksp. Teor. Fiz. **94**, 312–321 (September 1988)

The Faraday effect is used to investigate low-amplitude induced vibrations of a monopolar 180-degree domain wall in single-crystal yttrium iron garnet plates. Oscillations of the frequency dependence of the magneto-optic signal intensity are observed and are due to excitation of flexural standing waves of the wall along the sample thickness. The dispersion law and the characteristics of the spin waves localized in the wall are determined for the first time ever. Their dependence on the amplitude of the exciting field is found. Possible causes of a number of contradictions between the predictions of the existing theories and the experimental data are discussed. It is shown that some of the observed discrepancies can be qualitatively explained by taking magnetic aftereffect into account.

Interest in systems of lower dimensionality has increased in recent years. It is known that such objects can offer unique promise for the solution of most important fundamental and practical problems. The magnetic properties of one- and two-dimensional systems have not yet been extensively investigated. Recent experiments, nonetheless, have revealed a number of unusual phenomena in the behavior of spins localized in semiconductor dislocation cores<sup>1</sup> and in Bloch walls of magnetically ordered crystals.<sup>2–5</sup> Thus, the predicted excitation of solitary waves (dynamic solitons) was observed in a 180-degree domain wall (DW) in an yttrium iron garnet, as well as resonant generation and drift of Bloch lines in an alternating magnetic field. The micromechanism of these effects has not yet been explained. It is obvious, however, that they should be determined by spectrum singularities of magnons localized in the wall, by their interaction with Bloch lines, and also by formation of specific nonlinear waves via magnon binding. Study of the spectrum of DW elementary excitations is necessary also for the development of a microscopic theory of the mechanism that limit the wall mobility.<sup>6</sup> The information gained can be also of practical interest in view of the start of extensive research into the use of DW and of Bloch lines for the development of magnetic memory elements with ultrahigh information-recording density.<sup>7,8</sup>

The domain-wall elementary-excitation spectrum has heretofore been investigated only theoretically.<sup>9–14</sup> It has been shown, in particular,<sup>10,13,14</sup> that it can be asymmetric. Under nonstationary conditions the asymmetry might lead to the appearance of directed magnon flow along the DW and determine the aforementioned drift of the Bloch-line vibrations. Owing to the considerable experimental difficulties, however, the spectrum of magnons localized in DW has not yet been investigated. The possibility of performing such an experiment using a highly sensitive magneto-optic facility was first reported in Ref. 15. In the present paper we describe the results.

## PROCEDURE

The investigated objects were single-crystal yttrium-iron-garnet (YIG) slabs parallel to the (112) plane. The samples, in the form of a rectangular prism elongated along the [111] axis, contained one or two DW that separated domains with magnetization in the plane of the sample.

When such slabs were observed in polarized light, the DW were revealed by the Faraday effect in the form of light or dark stripes, depending on the polarity. In the absence of external fields in the equilibrium state, these boundaries were broken up into subdomains—sections with opposite rotation of the magnetization vector, separated by Bloch lines. Simultaneous application of a constant magnetic field ( $H_z$ ) perpendicular to the plane of the sample, and an alternating field ( $H_x$ ) parallel to the magnetization in the domain produced a monopolar DW,<sup>4</sup> which was in fact the object of our investigation.

To record the DW displacement, half the width of its image in a laser-illuminated polarization microscope (wavelength  $0.63 \mu\text{m}$ ) was bounded, as shown in the inset of Fig. 2, by a slit diaphragm and projected onto the photocathode of a photoelectron multiplier (PEM). The signal from the PEM, proportional to the DW displacement, was fed directly to the input of a selective microvoltmeter or to a sensitive narrow-band SK4-59 spectrum analyzer (SA) operating in the amplitude-frequency measurement mode. The uniform magnetic fields  $H_x$  and  $H_z$  were produced by Helmholtz coils. The amplitude of the alternating field  $H_x$  was maintained constant at all frequencies by a specially developed current-stabilization system that compensated for the field decrease, by the induction coils, at high frequency. The SA was scanned in frequency by the digital-analog converter of the "MERA CM-3A" computer, which averaged the signal, entered the spectrum into the memory, and computed the data and fed them to a telemonitor or an automatic plotter. Owing to the narrow band of the SA (100 Hz), and also to averaging over many points (1–10 thousand), it was possible to increase substantially the signal/noise ratio and the sensitivity of the facility, so that very small DW displacements ( $\sim 5 \text{ nm}$ ) could be recorded.

## RESULTS AND DISCUSSION

Figure 1 shows the dependences of the intensity  $I$  of the magneto-optic signal due to forced oscillations of a monopolar DW on the frequency  $\nu$  of the alternating magnetic field, measured at different values of the field amplitude  $H_x^0$  and at different SA sensitivities. All curves show clearly oscillation intensities in the form of a large assembly of practically equidistant peaks. Their number, position, and relative heights depended strongly on the alternating-field amplitude.

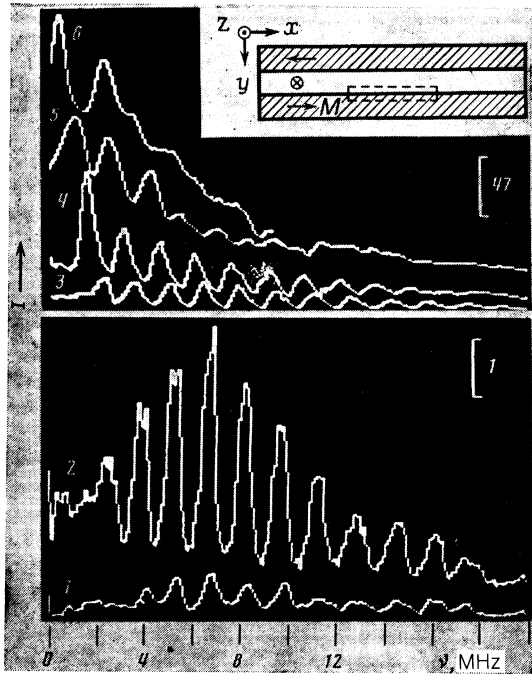


FIG. 1. Intensity  $I$  of the magneto-optic signal vs the frequency  $\nu$  of a sinusoidal field  $H_x$  for  $H_x^0 = 0.25$  mOe (1), 0.5 (2), 5 (3), 12.5 (4), 50 (5), 62.5 (6) and  $H_z = 28$  Oe (the scales of curves 3–6 are 47 times smaller than those of curves 1 and 2). All the curves were fed from the computer memory to a telemonitor and separated vertically. The dashed lines in the inset show the location of the photometered section.

On decrease of  $H_x^0$ , all the  $I(\nu)$  peaks were displaced as a unit towards higher frequencies, with vanishing of the first peak observed for the weakest exciting fields (curve 1). In these fields the heights of the peaks varied nonmonotonically with increasing serial number of the peak, passing through a maximum (e.g., at  $\nu \approx 7$  MHz on curve 2 of Fig. 1) that shifted to the left all the way to the first peak (curve 4). At large field amplitudes ( $\approx 50$  mOe), the depths of the oscilla-

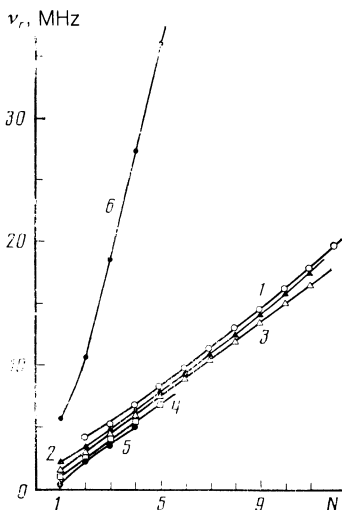


FIG. 2. Resonance frequency  $\nu_r$  of the peak vs its number  $N$  at  $H_z = 28$  Oe and  $H_x^0 = 0.25$  mOe (1), 5 (2), 12.5 (3), 25 (4), 50 (5), 6—calculated from (6) and plotted in accordance with  $n = N - 1$ .

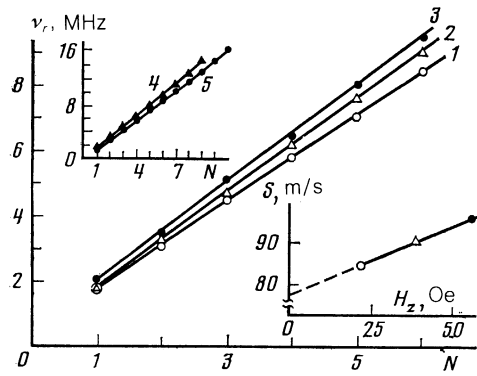


FIG. 3. Plots of  $\nu_r(N)$  measured at  $H_x^0 = 6.6$  mOe and  $H_z = 22.6$  Oe (1), 39.6 (2), 56.7 (3). Upper inset— $\nu_r(N)$  dependences for neighboring DW at  $H_x^0 = 52$  mOe and  $H_z = 23$  Oe. Lower inset—dependence of  $s = 2d\Delta\nu_r/\Delta N$  on the field  $H_z$  calculated on the basis of curves 1–3 ( $d = 32 \mu\text{m}$ ).

tions of the magneto-optic signal became significantly weaker and the high-frequency peaks were almost completely suppressed (curves 5 and 6). In the same fields, at  $\nu = 0.1$ –4 MHz, the mechanisms generating the Bloch-line, as well as their motion, were already patently nonlinear.<sup>4</sup>

Figure 2 shows the dependences of the resonance frequencies ( $\nu_r$ ) corresponding to the maxima of the intensity  $I_r$  at the peaks, on their number ( $N$ ), plotted for different  $H_x^0$ . It can be seen that they shift downward with increase of the exciting-field amplitude. Only curve 3 is a straight line, all others are clearly nonlinear. The slope of  $\nu_r(N)$  depended on the constant magnetic field  $H_z$ . It must be specially emphasized that the reversal of the sign of  $H_z$  which reversed the polarity of the DW, also changed the slope of  $\nu_r(N)$ . This slope differed also for neighboring DW (upper inset of Fig. 3). The  $\nu_r(N)$  dependence remained practically unchanged when the sample was shortened and when the photometry unit was displaced along the DW. However, decreasing the slab thickness ( $d$ ) (by mechanical polishing) changed noticeably the slope of  $\nu_r(N)$  in inverse proportion to  $d$  (Fig. 4). We note, finally, that the magneto-optic signal vanished when the photometry unit was moved outside the

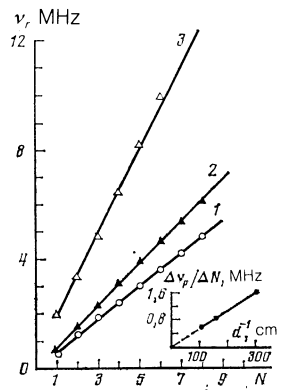


FIG. 4. Plots of  $\nu_r(N)$  measured for successively decreasing slab thicknesses at  $d = 90 \mu\text{m}$  (1), 64 (2), 30 (3);  $H_x^0 = 43$  mOe, and  $H_z = 28$  Oe. Inset: dependence of the slopes of the straight lines on  $d^{-1}$ .

width ( $\Delta = 2-3 \mu\text{m}$ ) of the optical image of the boundary, and the amplitude of the forced vibrations of the wall did not exceed  $\Delta/2$  even in the strongest of the investigated fields.

We proceed now to a discussion of the results. The oscillatory character of the  $I(\nu)$  dependence (Fig. 1) and the changes of the positions of the resonance peaks of  $\nu_r(N)$  with decrease of the sample thickness (Fig. 4) indicate that the decisive contribution to the mechanism that produces the described effect introduce flexural waves of the DW about an axis parallel to the direction of the magnetization in neighboring domains and to the crystal surface. In fact, the maximum amplitudes of the vibrating wall sections, which produce the maxima of the magnetooptic signal, correspond in this case to standing waves along the sample thickness. The frequencies ( $\nu_n$ ) of these special inhomogeneous DW vibrations are inversely proportional, in the simplest case of a linear dispersion law, to the wall dimension  $d$  in the direction perpendicular to the plate surface, and are linear in the number  $n$  of the half-waves spanned by the sample thickness:  $\nu_n = \omega_n/2\pi = sk_n/2\pi = sn/2d$  ( $s$  is the phase velocity and  $k_n$  is the wave number). This is precisely the character of the  $\nu_r(d)$  dependence observed in the experiment.

The frequencies  $\nu_r$  correspond thus to the frequencies of the vibration of the wall, in which they form standing waves, and the  $\nu_r(N)$  dependence reflects in fact the dispersion law  $\omega_n(k_n)$  of the spin waves localized in the DW. In the general case, as shown by theoretical calculations,<sup>9</sup> this law can also be nonlinear and have a gap indicative of the frequency of the homogeneous resonance of the DW displacement. The experimental  $\nu_r(N)$  plots (Fig. 2) indicate that the spectrum of the magnons localized in the wall depends noticeably on the amplitude of the magnon-exciting field. Let us show that to explain the experimental data it is necessary to take into account the magnetic aftereffects heretofore disregarded in the theories of elementary DW excitation.

We estimate first the character of the spectrum of DW vibrations in the potential well due to only the demagnetizing field that resists the motion of the wall by a force proportional to its displacement  $q$  from the equilibrium position. We use for this purpose the Landau-Lifshitz equations which were linearized and integrated by Slonczewski<sup>7</sup> over the wall thickness, as applied to a uniaxial magnet:

$$\psi_t = \gamma H + \frac{\sigma_0 \gamma}{2M} \nabla^2 q - \frac{\alpha}{\Delta_0} q_t, \quad (1)$$

$$\frac{q_t}{\Delta_0} = \frac{l}{2} \pi \gamma H_z + 4\pi M \gamma \psi - \frac{2\gamma A}{M} \nabla^2 \psi + \alpha \psi_t, \quad (2)$$

where  $q$  is the coordinate of the DW center on the  $y$  axis normal to its plane,  $\nabla^2 q = q_{zz}$  (we are considering waves propagating along the  $z$  axis which is perpendicular to the plane of the slab),  $\psi$  is the azimuthal angle at which the magnetization ( $\mathbf{M}$ ) emerges from the DW plane,  $\alpha$  is the damping parameter in the Gilbert form,  $\Delta_0 = (A/K)^{1/2}$ ,  $\sigma_0 = 4(AK)^{1/2}$ ,  $A$  and  $K$  are the exchange and anisotropy constants,  $\gamma$  is the gyromagnetic ratio,  $H = H_x - \kappa_0 q/2M$ , and  $\kappa_0$  is the restoring-force coefficient.

Eliminating  $\psi$  from (1) and (2), we obtain in the long-wave approximation, for  $\alpha \ll 1$ , the equation

$$q_{tt} - s^2 q_{zz} + \Omega_\alpha q_t + \Omega_0^2 q = \frac{2MH}{\kappa_0} \Omega_0^2, \quad (3)$$

where

$$s = s_0(1 \pm H_z/8M \pm h)^{1/2}, \quad s_0 = (\sigma_0/m)^{1/2}, \quad m = (2\pi\Delta_0\gamma^2)^{-1}, \\ h = \kappa_0\Delta_0/8\pi M^2, \quad \Omega_\alpha = \omega_\alpha(1 \pm H_z/8M \pm h), \\ \omega_\alpha = 4\pi M\alpha\gamma, \quad \Omega_0 = \omega_0(1 \pm H_z/8M)^{1/2}, \quad \omega_0 = (\kappa_0/m)^{1/2}.$$

The  $+$  and  $-$  signs are valid respectively in the expressions for  $s$  and  $\Omega_\alpha$  if  $H_z/8M + h \gtrless -1$ , and for  $\Omega_0$  if  $H_z/8M \gtrless -1$ .

The solution (3) depends, naturally, on the boundary conditions. We assume, on the basis of direct observations of the long-distance DW displacements, that under the conditions of the described experiment there was no pinning of the DW on the slab surface ( $q_z(0) = q_z(d) = 0$ ). Flexural vibrations of a DW in a uniform field  $H_x$  could be excited, for example, by the action of a non-uniform internal field due to crystal-lattice defects and, in particular, to the sample surface. For solutions in the form

$$q = \sum_n q_n \cos(k_n z) e^{i\omega t} \quad (4)$$

we obtain

$$q_n(\omega) \sim \left\{ \left[ 1 - \frac{\omega^2}{\Omega_0^2} + \left( \frac{sk_n}{\Omega_0} \right)^2 \right]^2 + \left( \frac{\Omega_\alpha \omega}{\Omega_0^2} \right)^2 \right\}^{-1/2}, \quad (5)$$

$$\omega_n^2 = \Omega_0^2 - \Omega_\alpha^2/2 + (sk_n)^2. \quad (6)$$

This result differs from that of Winter<sup>9</sup> in that the parameters in (6) depend on  $H_z$ . Note that the validity of Eqs. (1) and (2) is restricted by the conditions  $k\Delta_0 \ll 1$  and  $K \gg 2\pi M^2 \sin^2 \psi$  (Ref. 16). In the case of a weakly anisotropic magnet ( $K \ll 2\pi M^2$ ) expression (6) can therefore describe only DW vibrations of small enough amplitude.

Let us compare the experimental data with the foregoing calculation results. Since there are no sufficient grounds for an unambiguous identification of the peak numbers, we analyze the assumption (different from that set forth in Ref. 15) that all the modes of the flexural DW vibrations ( $n = 0, 1, 2, \dots$ ) were excited in the experiment, and the frequency ( $\nu_1$ ) of the first peak on the  $I(\nu)$  plots (Fig. 1) corresponded to a translational mode (to a uniform resonance of wall displacement as a whole:  $k_n = 0$ ). This corresponds in Fig. 2 to curve 6 calculated from Eq. (6). The experimental values of  $\nu_1$  turn out to be considerably lower than that calculated (5.7 MHz) using the measured value  $\kappa_0 = 7.8 \cdot 10^4 \text{ G/s}^2 \cdot \text{cm}^2$ . It is seen from the data of Fig. 2 that the frequency of the first resonance peak changes from 0.4 to 2.6 MHz when the alternating-field amplitude decreases from 50 to 5 mOe, i.e., the size of the gap in the spectrum depends on the amplitude of the DW vibrations.

The experimentally observed dependence of the phase velocity  $s$  of the flexural DW waves on the constant field  $H_z$  (Fig. 3) turns out to be much stronger than the calculated one. Nor is there agreement between the phase velocities themselves: the calculated ( $s_0 = 570 \text{ m/s}$ ) and the experimental ( $s_0 = 76 \text{ m/s}$ ), obtained by extrapolation of the  $s(H_z)$  dependence to zero  $H_z$  (Fig. 3).

It was shown in Refs. 10, 13, and 14 that a more rigorous allowance for the magnetodipole interactions leads to asymmetry of the spin-wave spectrum in DW ( $\omega(k) \neq \omega(-k)$ ). The value of the phase velocity for the

forward wave ( $\sim 60$  m/s), calculated on the basis of Eq. (24) of Ref. 13, turns out to be very close to the experimentally measured value. For the backward wave, the calculated value exceeds it by more than two orders. On the other hand, the experimentally observed difference between the phase velocities in neighboring DW, or the change of  $s$  when the wall polarity is reversed (this could be regarded as a manifestation of spectrum asymmetry) was small compared with the absolute value of  $s$ .

The best quantitative agreement between theory and experiment is observed for the parameter  $\alpha$ . Its value, calculated using the measured width of the lowest-frequency peak ( $\Delta\nu$ ) at 0.7 maximum level  $\alpha = \Omega_\alpha/4\pi M\gamma = \Delta\nu/2M\gamma = (0.6 \pm 0.2) \cdot 10^{-4}$ , was practically equal to the ( $\alpha = 0.7 \cdot 10^{-4}$ ) calculated from the FMR linewidth. In a number of cases the peak width, meaning also  $\alpha$ , increased (approximately doubled) when  $N$  was increased from 1 to 12; this may be a manifestation of the dispersion in the damping of the flexural waves.<sup>17</sup>

Thus, the comparison shows that a number of qualitative and quantitative discrepancies can be discerned between the prediction of the theory<sup>7,9,10,13,14</sup> and experiment. It is impossible, in particular to explain the nonmonotonic dependence of the peak height on its number and the suppression of the first peak, which were observed in the weakest fields, as well as the increase of the resonance frequencies  $\nu_r(N)$  with decrease of  $H_x^0$  (Fig. 1). It follows from Eq. (5) that the transition from the resonant to the relaxation form of the  $q_n(\omega)$  curve may be due to the increased damping ( $\Omega_\alpha$ ) or the decreased damping  $\Omega_0$ , for which the peak frequency should decrease according to (6). Experiment, however, shows an increase of the resonance frequencies  $\nu_r(N)$  with decrease of  $H_x^0$ .

These effects can be explained by taking into account the magnetic aftereffect determined by the interaction of the moving DW with crystal-lattice point defects whose state depends on the magnetization direction<sup>18</sup> (the appearance of such effects for free DW vibrations in the investigated YIG was reported by us earlier<sup>5</sup>). The equilibrium distribution of such defects near the DW is the source of the local induced anisotropy (with a characteristic spatial scale on the order of the DW thickness and with a relaxation time  $\tau$ ), which stabilized the specified distribution of  $\mathbf{M}$ . Consequently, low-amplitude DW vibrations will take place in a deeper potential well than vibrations with large amplitudes. The well influence on the DW motion can be described with the aid of the effective pressure<sup>18</sup>

$$P(q, t) = \int_{-\infty}^t \frac{\partial W(q-q')}{\partial q} \frac{e^{(t-t')/\tau}}{\tau} dt',$$

where  $W(q-q')$  is the energy of the induced anisotropy that determines the local potential well for the DW. In weak fields it suffices to use the parabolic-potential-well approximation:

$$W(q-q') = \kappa(q-q')^2/2, \quad (7)$$

where  $\kappa$  is a coefficient that characterizes the restoring force in the well. Adding to the right-hand side of Eq. (3) the term  $P(q, t)/m$ , we obtain after simple transformations the modified equation of motion

$$q_{ttt} + (\Omega_\alpha + 1/\tau)q_{tt} + [\Omega_0^2(1+\eta) + \Omega_\alpha/\tau]q_t + (\Omega_0^2/\tau)q - s^2q_{zzt} - (s^2/\tau)q_{zz} = (2M/\kappa_0)(H_t + H/\tau)\Omega_0^2, \quad (8)$$

where  $\eta = \kappa/\kappa_0$ . From this we obtain for solutions of type (4):

$$q_n(\omega) \sim (1 + \omega^2\tau^2)^{-1/2} / \left\{ \left[ 1 - \frac{\omega^2}{\Omega_0^2} (1 + \Omega_\alpha\tau) + \left( \frac{sk_n}{\Omega_0} \right)^2 \right]^2 + \omega^2\tau^2 \left[ 1 + \eta + \frac{\Omega_\alpha}{\Omega_0^2\tau} + \left( \frac{sk_n}{\Omega_0} \right)^2 - \frac{\omega^2}{\Omega_0^2} \right]^2 \right\}^{1/2} \quad (9)$$

Figure 5 shows  $\omega_n(k_n)$  plots calculated with a computer from (9) for different values of  $\eta$  in the case  $\Omega_0\tau = 1$ . It can be seen that with increase of  $\eta$  the frequencies of the zeroth resonance peak ( $n=0$ ) and for the others ( $n \neq 0$ , for which  $\omega_n\tau$  becomes  $> 1$ ) increase. In addition, as seen from the upper inset of Fig. 5, which contains the  $q_n(\omega)$  curves for different  $\eta$  at two fixed values of  $k_n$ , the height of each peak decreases with increase of  $\eta$ , and the relaxation section becomes ever more pronounced to the left of the first peak. From a comparison of curves 6–8 with curves 9–11, calculated for the same values of  $\eta$  but for larger  $k_n$ , it can be seen that with increase of  $k_n$  the dependence of the peak height on  $\eta$  becomes weaker. This circumstance can, in particular, determine the experimentally observed nonmonotonic dependence of the peak height on its number. The lower inset of Fig. 5 shows relative intensities of three different peaks for  $\eta = 5$ . Calculations have shown that with decrease of  $\eta$  the peak having the maximum height had continuously lower values of  $n$ .

With increase of  $\tau$  (in the region  $\Omega_0\tau > 1$ ), the dependence of  $\omega_n$  and  $q_n$  on  $\eta$  weakens, but remains qualitatively the same as in Fig. 5. For shorter relaxation times ( $\Omega_0\tau < 1$ ), however, a fundamental difference sets in, such that at certain values of  $\eta$  the resonances on the  $q_n(\omega)$  curves vanish completely. In Fig. 6, which shows the calculated values of  $q_n(\omega)$  and  $\omega_n(k_n)$  at  $\Omega_0\tau = 0.1$ , there are no values of  $\omega_n$

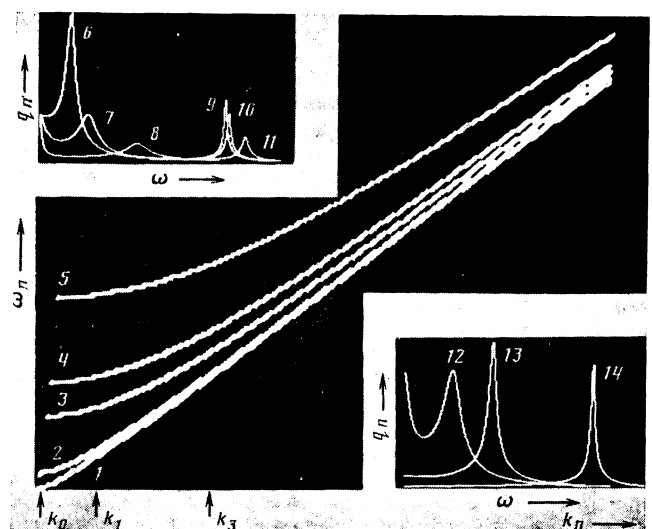


FIG. 5. Dispersion curves  $\omega_n(k_n)$  calculated on the basis of (9) for  $\Omega_0\tau = 1$ ,  $\Omega_0 = 1.5$  MHz,  $\Omega_\alpha = 0.2$  MHz,  $\pi s/d = 6$  MHz and  $\eta = 0$  (1), 50 (2), 100 (3), 300 (4), 500 (5). The insets show the  $q_n(\omega)$  curves calculated from (9): top—for  $\eta = 1$  (6, 9), 5 (7, 10), 25 (8, 11) and  $k_n$  (6, 7, 8), 9 (9, 10, 11); bottom—for  $\eta = 5$ ,  $k_0$  (12),  $k_1$  (13),  $k_3$  (14).

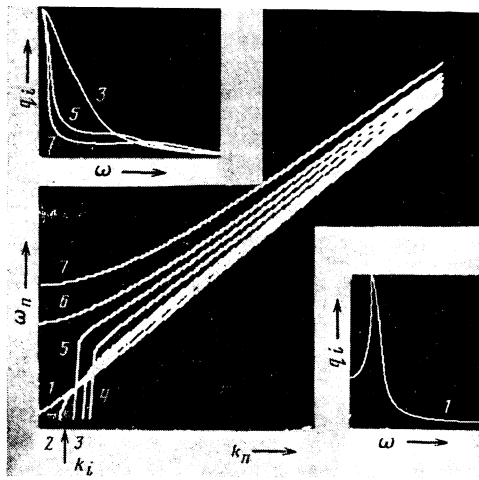


FIG. 6. Dispersion curves  $\omega_n(k_n)$  calculated for  $\Omega_0\tau = 0.1$ ,  $\Omega_0 = 1.5$  MHz,  $\Omega_n = 0.2$  MHz and  $\eta = 0$  (1), 30 (2), 50 (3), 100 (4), 150 (5), 200 (6), 300 (7). Inset— $q$ , calculated for  $k = k_n$  and the same values of  $\eta$  as  $\omega_n(k_n)$ .

(in the region of the smallest  $k_n$ ) for  $k_n$  corresponding to such nonresonant  $q_n(\omega)$ . The  $q_n(\omega)$  curves have a relaxation form for these values of  $k_n$ , and a resonance form for all others.

The above changes of the experimental  $I(\nu)$  and  $\nu_r(N)$  dependences with increase of  $H_x^0$  (Figs. 1 and 2) agree qualitatively with the above calculations, if one makes the natural assumption that with decrease of the DW vibration amplitude the depth of the potential well (meaning also the parameter  $\eta$ ) has increased. It is impossible, however, to obtain on the basis of the considered approximation a quantitative agreement between the calculated and measured characteristics ( $s, \omega_0$ ) of the spin-wave spectrum. To obtain agreement it is obviously necessary to take into account also the influence exerted on the DW structure by the point defects that determine the influence of the magnetostatic-interaction aftereffect that appears in the case of flexural vibrations of the wall and is due to the limited size of the sample and also to cubic magnetic anisotropy.

As to the singularities of the DW vibrations in strong exciting fields (Fig. 1, curves 5 and 6), we note only that the most effective limitation of the DW resonant-vibration amplitude (suppression of the peaks) occurred at those frequencies for which creation and annihilation of Bloch lines were no longer observed. It appears that in this case it is necessary to take into account not only the formation of nonlinear excitations in the wall<sup>5,6,19</sup> (i.e., the inhomogeneous precession of the magnetization in the DW), but also the homogeneous ("Walker") precession of  $\mathbf{M}$  at large angles, since the amplitude  $H_x^0$  was close to the critical Walker field<sup>7</sup>  $H_w = 2\pi M\alpha \approx 60$  mOe.

## CONCLUSION

As a result of our investigations of small domain-wall vibrations in YIG we have thus revealed resonances due to standing DW flexure waves over the sample thickness. By investigating a material that has the lowest possible FMR width, and hence a small damping parameter, we succeeded in effectively exciting and recording a rather large number of resonances. This enabled us to investigate in detail, for the first time ever, the dispersion of spin waves localized in a Bloch wall and their principal characteristics, viz., damping, phase velocity, and gap. It turned out that the spectrum of flexural DW waves can undergo substantial changes, depending on the amplitude of the exciting alternating field, and also on the intensity and sign of the constant field  $H_z$  that stabilizes the monopolar state of the wall.

We have shown that the existing linear theories, developed for uniaxial magnets, cannot explain consistently the experimental data. A number of effects revealed in the very weakest exciting fields could be qualitatively described on the basis of a model that takes into account the magnetic after effect. Further development of the theory is needed to eliminate the quantitative discrepancies between the measured and calculated values of the characteristics of the spectrum of magnons localized in a wall, and also to explain the nonlinear effects observed in strong exciting fields.

<sup>1</sup>V. A. Grazhulis and Yu. A. Osipyan, Zh. Eksp. Teor. Fiz. **60**, 1150 (1971) [Sov. Phys. JETP **33**, 623 (1971)].

<sup>2</sup>V. N. Nikitenko, L. M. Dedukh, V. S. Gornakov, and Yu. P. Kabanov, Pis'ma Zh. Eksp. Teor. Fiz. **32**, 402 (1980) [JETP Lett. **32**, 377 (1980)].

<sup>3</sup>V. S. Gornakov, L. M. Dedukh, Yu. P. Kabanov, and V. I. Nikitenko, Zh. Eksp. Teor. Fiz. **82**, 2007 (1982) [Sov. Phys. JETP **55**, 1154 (1982)].

<sup>4</sup>V. S. Gornakov, L. M. Dedukh, and V. I. Nikitenko, *ibid.*, **86**, 1505 (1984) [**59**, 881 (1984)].

<sup>5</sup>V. S. Gornakov, L. M. Dedukh, V. I. Nikitenko, and V. T. Synogach, *ibid.*, **90**, 2090 (1986) [**63**, 1225 (1986)].

<sup>6</sup>A. S. Abyzov and B. A. Ivanov, *ibid.*, **76**, 1700 (1976) [**49**, 865 (1976)].

<sup>7</sup>A. P. Malozemoff and J. C. Slonczewski, *Magnetic Domain Walls in Bubble Materials*, Academic, 1979.

<sup>8</sup>S. Konishi, IEEE Trans. **MAG-19**, 1838 (1983).

<sup>9</sup>J. M. Winter, Phys. Rev. **124**, 452 (1961).

<sup>10</sup>J. F. Nanak, Phys. Rev. **134**, A411 (1964).

<sup>11</sup>M. M. Farztdinov and E. A. Turov, Fiz. Met. Metallov. **29**, 458 (1970).

<sup>12</sup>M. I. Kurkin and A. P. Tankeev, *ibid.*, **36**, 1149 (1973).

<sup>13</sup>I. A. Gilinskii, Zh. Eksp. Teor. Fiz. **68**, 1032 (1975) [Sov. Phys. JETP **41**, 511 (1975)].

<sup>14</sup>A. E. Borovik, V. S. Kuleshov, and M. A. Strzemechnyi, *ibid.*, **68**, 2236 (1975) [**41**, 1118 (1975)].

<sup>15</sup>L. M. Dedukh, V. I. Nikitenko, and V. T. Synogach, Pis'ma Zh. Eksp. Teor. Fiz. **45**, 386 (1987) [JETP Lett. **45**, 491 (1987)].

<sup>16</sup>J. C. Slonczewski, Intern. J. Magnetism **2**, 85 (1972).

<sup>17</sup>V. G. Bar'yakhtar, Zh. Eksp. Teor. Fiz. **87**, 1501 (1984) [Sov. Phys. JETP **60**, 863 (1984)].

<sup>18</sup>A. Hubert, *Theorie d. Domänwände in geordneten Medien*, Springer, 1974.

<sup>19</sup>A. K. Zvezdin, V. V. Kostyuchenko, and A. F. Popkov, Fiz. Tverd. Tela (Leningrad) **27**, 2936 (1985) [Sov. Phys. Solid State **27**, 1765 (1985)].

Translated by J. G. Adashko